Synthesis, Crystal Structure and Spin-Orbit Coupling Analysis for Mono-Scorpionate Eu(III) Complexes

Kira E. Vostrikova * , Taisiya S. Sukhikh , Alexander N. Lavrov

Posted Date: 25 August 2023

doi: 10.20944/preprints202308.1806.v1

Keywords: europium(III) complexes; scorpionate; tripodal ligand; trispyrazolylmethane; tris(3,5-dimethyl-1-pyrazolyl)methane; magnetic properties; spin-orbit coupling

Article

Synthesis, Crystal Structure and Spin-Orbit Coupling Analysis for Mono-Scorpionate Eu(III) Complexes

Kira E. Vostrikova *, Taisiya S. Sukhikh and Alexander N. Lavrov

Nikolayev Institute of Inorganic Chemistry SB RAS, 3 Akad. Lavrentiev Ave., Novosibirsk 630090, Russia; sukhikh@niic.nsc.ru (T.S.S.), lavrov@niic.nsc.ru (A.N.L.)

* Correspondence: vosk@niic.nsc.ru

Abstract: Complexes of triply positive europium ion with organic ligands are popular objects for studying photophysical properties. This is related not only to the bright red emission of this 4f element, but also to some spectroscopic peculiarities of its luminescence: the first excited spin-orbit level ($^7F_1$) lies only about 300 cm^{-1} above the ground state ($^7F_0$), so that at room temperature its population is around 25–30%. However, such electronic structure of Eu(III) provides its paramagnetism under ordinary conditions. This fact is often ignored by researchers, which is shortsighted from the materials science point of view. A comprehensive and systematic study of the magnetic behavior for the Eu(III) molecular coordination compounds is a challenging task for the development of new polyfunctional materials. The present work presents synthesis, single crystal XRD analysis results, and a magnetic study for the firstly prepared europium(III) complexes with two neutral scorpionate ligands: trispyrazolylmethane ($HCPz_3$) and its methylated analog, tris(3,5-dimethyl-1-pyrazolyl)methane ($HC(Pz^{Me_2})_3$). The values of the spin-orbit coupling parameter obtained for Eu-trication by a theoretical approximation of the experimental magnetic susceptibility data are compared with those known for the scarce amount of the magnetically studied molecular compounds.

Keywords: europium(III) complexes; scorpionate; tripodal ligand; trispyrazolylmethane; tris(3,5-dimethyl-1-pyrazolyl)methane; magnetic properties; spin-orbit coupling

1. Introduction

The design of molecular materials with newly developed functionalities holds potential for technological advances. Switchable by different stimuli molecules are appealing model compounds due to their potential for electronic handling. This requires implementation of diverse physical properties within monophasic materials designable at the molecular level. As the result, such materials should become the tool for optical, magnetic, electronic, and multifunctional devices linking high performance with extreme miniaturization. For these purposes, realizing how the fundamental properties of molecular coordination compounds arise and how they can be controlled is very important for the creation of new functional molecular materials.

The unique electronic and physical properties of rare earth ions have been utilized for a variety of applications, including magnetic and luminescent materials. The focus in this direction is on luminescent single-molecule magnets (SMMs) searching for rational synthetic approaches resulting in strong magnetic anisotropy and enhanced photoluminescence since the latter can be used to probe the electronic structure of lanthanide based SMMs deposited on a surface [1,2].

The most common are the lanthanide (Ln) compounds in which the metal ion is in the trivalent state, and the redox activity in lanthanide complexes is usually limited to the ligand. However, lanthanide-based redox activity is also possible. Among the divalent lanthanides, europium possesses the most reachable divalent oxidation state, Eu^{2+}, because of its half-filled $4f^7$ electronic configuration and, therefore, a high stabilization from exchange energy [3,4]. For this reason in a vast majority of the magnetically studied Eu^{3+} molecular complexes, their magnetic susceptibility experiences an increase at near liquid helium temperatures since the presence a tiny amount of Eu^{2+} impurity [5,6].

Preprints (www.preprints.org) | NOT PEER-REVIEWED | Posted: 25 August 2023 doi:10.20944/preprints202308.1806.v1

To date, there is abundant information on the photophysical properties of Eu^{3+} molecular complexes, which are quite well studied spectroscopically. However, due to the non-magnetic ground term ^7F ($S = L = 3$) of the ion, researchers often leave the magnetic properties of europium luminescent compounds unattended. Although due to the thermal population of the excited states, Eu^{3+} becomes noticeably paramagnetic already at 100 K, reaching a value of effective magnetic moment of ~ 3.2 μ_B at room temperature. Given the low redox potential of the Eu^{2+}/Eu^{3+} pair [7], which in combination with non-innocent organic ligands can lead to interesting both photo- and magnetically switchable materials, including SMMs [8,9].

Tuning the electronic properties of a compound is the most common challenge for materials scientists. This can be achieved by varying the ligand environment of the central atom, namely the geometry of the polyhedron and the ligand field strength. The latter is mainly determined by the nature of the donor atoms, whereas the former depends not only on the geometry of the ligand but also on the predictable way in which it is coordinated. Organic tripod molecules having donor atoms on each of the three legs are the most prospective for the chemical construction of various complexes with a prescribed geometry. Moreover, the latter can be easily adjusted by methods of synthetic organic chemistry.

Previously, we have obtained the monoradical, $[LnRad(NO_3)_3]$ (Ln^{3+} = Gd, Tb, Dy, Tm [10], and biradical $[Ln(Rad)_2(OTf)_3]$ (Ln^{3+} = Eu and Dy) [11] complexes, where Rad is a tripodal nitroxyl radical (Scheme 1(a)), 4,4-dimethyl-2,2-bis(pyridin-2-yl)-1,3-oxazolidine-3-oxyl. We were somewhat surprised by molar magnetic susceptibility values of 1.78 and 0.348 emuK/mol at 300 and 2 K respectively for the biradical complex, comparing them with those of $[Eu(radical)_2(anion)_3]$ compounds [12–18]. In this series, they were varied from 1.93 to 3.09 emu K/mol at room temperature, and from 0.035 to 0.42 emuK/mol at low temperature. Analyzing the literature data for known Eu^{3+} biradical complexes, we have noticed that the rough estimates of magnetic parameters values for such systems resulted in a large scatter in values of λ, spin-orbit coupling (SOC) parameter.

It should also be pointed out that there is no reasonable explanation for the underestimated magnitudes of the molar magnetic susceptibility of $[Eu(radical)(anion)_3]$ complexes at low temperature (0.192÷0.252 instead of 0.375 emuK/mol) [19–21] when a singlet state is operative for Eu^{3+}. These two facts are most likely due to the lack of models to account for the strong spin-orbit coupling (SOC) for the Eu^{3+} complexes with paramagnetic ligands. In addition, preliminary magnetic studies of the isomorphic analogue $[EuRad(NO_3)_3]$ did not clarify the situation with the underestimation of the low-temperature $\chi_M T$ value for the monoradical europium complexes mentioned above, since the value of $\chi_M T$ for $[EuRad(NO_3)_3]$ at 2 K lies in the same range. Considering that the Ln–Rad antiferromagnetic coupling found for the $[GdRad(NO_3)_3]$ complex is –23 cm^{-1} [10], an ambient temperature $\chi_M T$ value for $[EuRad(NO_3)_3]$ can be estimated as a sum of the contributions of the uncorrelated radical (0.375 emuK/mol) and $[EuL_{dia}(NO_3)_3]$. The latter is a model complex of a diamagnetic tripodal ligand possessing a coordination polyhedron geometry close to that of the radical complex. Such a strategy of diamagnetic substitution for obtaining information on the crystal field (CF) effects in paramagnetic Ln ions has been applied earlier [15,22,23]. This experimental approach aims to reveal the nature of the coupling between the radical and the lanthanide subtracting the CF splitting. This method was applied for two homologous series of complexes: $[LnNN^{trz}_2(NO_3)_3]$ and $[Ln(Nitrone)_2(NO_3)_3]$ [15]; $[Ln(HBPz_3)_2SQ]$ and $[Ln(HBPz_3)_2Trp]$ [22,23]. Where NN^{trz} is 2-(4′,5′-dimethyl-1′,2′,3′-triazolyl)-4,4,5,5-tetramethyl-4,5-dihydro-1H-imidazolyl-1-oxy-3-oxide, and SQ is 3,5-di-tert-butylsemiquinonato respectively, while the diamagnetic homologue ligands, Nitrone and Trp are 3-N-tert-butylnitrone-4,5-dimethyltriazole and tropolonate correspondingly.

To determine the reference values of the magnetic susceptibility of Eu(III) complexes with diamagnetic tripodal ligands with similar geometry of the coordination polyhedron, we synthesized and magnetically studied three Eu^{3+} complexes comprising diamagnetic tripodal ligand depicted in Scheme 1.

Preprints (www.preprints.org) | NOT PEER-REVIEWED | Posted: 25 August 2023 doi:10.20944/preprints202308.1806.v1

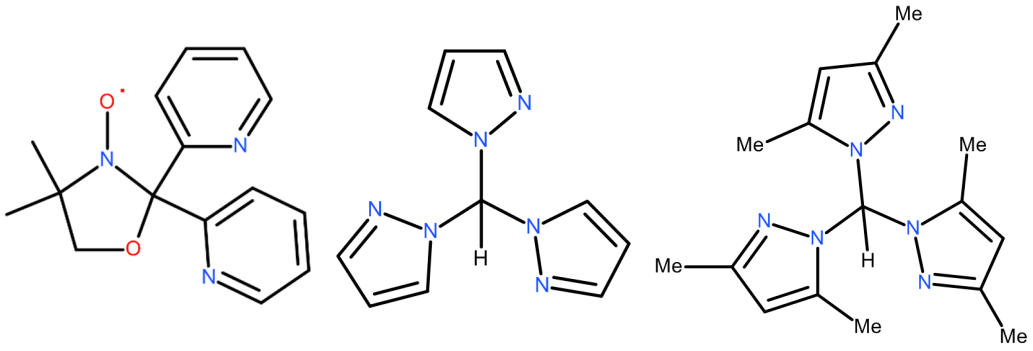

(**a**) (**b**) (**c**)

Scheme 1. The tripodal ligands: (**a**) 4,4-dimethyl-2,2-bis(pyridin-2-yl)-1,3-oxazolidine-3-oxyl (Rad); (**b**) Trispyrazolylmethane ($HCPz_3$); (**b**) tris(3,5-dimethyl-1-pyrazolyl)methane ($HC(Pz^{Me_2})_3$).

2. Short Theoretical Background

The trivalent europium ion (Eu^{3+}) shows an intense red photoluminescence upon irradiation with ultra violet radiation [24]. This luminescence is observed not only for Eu^{3+} ions doped into crystalline host matrices or glasses, but also for europium(III) complexes with organic ligands [25]. These ligands can act as an antenna to absorb the excitation light and to transfer the excitation energy to the higher energy levels of the Eu^{3+} ion, from which the emitting excited levels can be populated [2]. Not only its red luminescence, but also the narrow transitions in luminescence spectra are typical features of the Eu^{3+} ion [26], and these spectroscopic properties have been known from the earliest history of the chemical element europium [27]. Many Eu^{3+} compounds show an intense photoluminescence, due to the $^5D_0 \rightarrow {}^7F_J$ transitions (J = 0–6) from the $^5D_0$ excited state to the J levels of the ground term ^7F. The fine structure and the relative intensities of the transitions in luminescence spectra of Eu^{3+} can be used to probe the local surroundings of the europium. The spectroscopic experimental data provide information on the point group symmetry of the Eu^{3+} site and as well as on the polyhedron geometry [26], which it is especially useful for solution study. Other techniques (optical, magnetic or magneto-optical) can also be used for determination of the position and assignment of the CF energy levels inside the 4*f* shell: two-photon absorption, Zeeman spectroscopy and magnetic circular dichroism [24].

In the first approximation, a lanthanide ion in a molecular coordination compound behaves as a free-ion. The paramagnetic behavior of the tripositive Ln^{3+} ions is due to the presence of unpaired 4f-unpaired electrons. Since these electrons are shielded by the outer electronic closed shell, the spin-orbit interaction is believed to play a decisive role in their magnetic properties. Therefore, depending on the sign of the spin-orbit interaction, their total magnetic moments J defined as $J = L \pm S$, where L means the angular momentum and S – the spin momentum. It follows that the magnetic moment of the complex should indicate whether these 4f-electrons are involved in bond formation or not. For a majority of the Ln^{3+} ions, the $^{2s+l}L_J$ free-ion ground state (GS) is well isolated in energy from the first excited state. Therefore, only the GS is thermally populated in the temperature range of 0÷300 K. In the free-ion approximation the molar magnetic susceptibility for a mononuclear species is given by [28]

$$\chi_J = \frac{Ng_J^2\beta^2 J(J+1)}{3kT} + \frac{2N\beta^2(g_J - 1)}{3\lambda} \quad (1)$$

where λ is the spin-orbit coupling parameter and g_J is equal to

$$g_J = \frac{3}{2} + \frac{[S(S+1) - L(L+1)]}{2J(J+1)} \quad (2)$$

and L is the orbital quantum momentum. For J = 0 there is obviously no first-order Zeeman splitting. However, application of a magnetic field can result in second-order splitting and appearance of a net magnetic moment. The last part in (1) is a temperature independent contribution

Preprints (www.preprints.org) | NOT PEER-REVIEWED | Posted: 25 August 2023 doi:10.20944/preprints202308.1806.v1

arising from the coupling between the ground and excited states through the Zeeman perturbation. For Ln molecular compounds the $\chi_M T$ versus T curve often differs slightly from what is predicted by (1). This deviation occurs for two reasons: the crystal field, which partially removes the $2J + 1$ degeneracy of the GS in zero field, and the thermal population of Ln^{3+} excited states. The latter is most pronounced for tripositive samarium and europium, which possess excited states located close in energy to the ground one. In the case of europium, its ^7F ground term is split by the spin-orbit coupling into seven multiplets ($^7F_0$, $^7F_1$, $^7F_2$, $^7F_3$, $^7F_4$, $^7F_5$, $^7F_6$), whose energies are $E(J) = \lambda J(J + 1)/2$, where the energy of the $^7F_0$ ground state is taken as the origin. Since λ is small enough for the first excited states to be thermally populated, the magnetic susceptibility may be written as

$$\chi_M = \frac{\sum_{J=0}^{6}(J+1)\chi_J e^{-\frac{\lambda J(J+1)}{2kT}}}{\sum_{J=0}^{6}(2J+1)\chi_J e^{-\frac{\lambda J(J+1)}{2kT}}} \quad [28] \qquad (3)$$

where χ_J is given by equation (1). In the case of Eu^{3+}, all of the g_J are equal to 3/2, except g_0, which is equal to $2 + L(=2 + S) = 5$, *i.e.* $(\chi_M T)_{Eu}$ can be expanded as [29]:

$$\frac{N\beta^2}{3kx}\left[24 + \left(\frac{27}{2}x - \frac{3}{2}\right)e^{-x} + \left(135x - \frac{9}{2}\right)e^{-3x} + \left(189x - \frac{7}{2}\right)e^{-6x} + \left(405x - \frac{9}{2}\right)e^{-10x} + \left(\frac{1485}{2}x - \frac{11}{2}\right)e^{-15x} + \left(\frac{2457}{2}x - \frac{13}{2}\right)e^{-21x}\right] \qquad (4)$$
$$\left[1 + 3e^{-x} + 5e^{-3x} + 7e^{-6x} + 9e^{-10x} + 11e^{-15x} + 13e^{-21x}\right]$$

where $x = \lambda/kT$.

At moderate temperatures, owing to the value of λ ~ 350 cm^{-1} [28], only the first three lower states ($^7F_0$, $^7F_1$, $^7F_2$) having the energies 0, λ, and 3λ can be considerably populated; since the $^7F_0$ ground state is formally nonmagnetic, the lower limit of χT is zero. However, the low-temperature limit of the magnetic susceptibility, χ_{LT}, is nonzero due to the temperature-independent contribution arising from the coupling between the ground and excited states. According to equation (4) which acquires a very simple form in the $T = 0$ limit, the χ_{LT} value is directly related to λ as:

$$\chi_{LT} = 8N\beta^2/\lambda = (2.085 \times 10^{-3})/\lambda \ (\lambda \text{ in } cm^{-1}) \qquad (6)$$

Although the aforementioned description has proved to capture the key qualitative features of the magnetic susceptibility of Eu3+-based compounds, its performance turns out to be not as good when it comes to precise determination of λ and quantitative comparison with spectroscopic results. The problem stems from the crystal-field splitting of the excited $J \neq 0$ multiplets that has not been taken into account by the equation (4) [29–31] Given that the $^7F_1$ multiplet is the closest one in energy to the ground level, its splitting into three Stark sublevels plays the most important role. For example, when we consider the low-T magnetic susceptibility and take into account the splitting of the first excited multiplet, the equation (6) turns into:

$$\chi_{LT} = (8N\beta^2/3)(1/E_1+1/E_2+1/E_3) \qquad (7)$$

where E_1, E_2, E_3 are the energies of the $^7F_1$-multiplet Stark sublevels. Apparently, when the multiplet splitting is negligible, the eq. (6) and (7) are equivalent, as $1/E_1 = 1/E_2 = 1/E_3 = 1/\lambda$. But, in the opposite case of strong splitting, the average $(1/E_1+1/E_2+1/E_3)/3$ becomes significantly larger than $1/\lambda$, resulting in the magnetic susceptibility in the low-temperature plateau region to be enhanced in comparison with the values predicted by the eq. (4) [31].

3. Results and Discussion

3.1. Synthetic Aspects

As can be seen in Scheme 1, the paramagnetic tripod, Rad, has a close to its diamagnetic relatives organization of the organic molecule. Formally, it can be referred to methane derivatives, like the other two tripodal ligands, since for all three molecules the bridgehead atom is a carbon. In addition, despite the difference in the donor atoms on the legs of the paramagnetic tripod (oxygen atom from the nitroxyl group instead of the nitrogen of the pyrazole), it also forms three six-membered chelate cycles when coordinated.

Preprints (www.preprints.org) | NOT PEER-REVIEWED | Posted: 25 August 2023 doi:10.20944/preprints202308.1806.v1

Upon coordination of the neutral tripods, (tris(pyrazol-1-yl)methanes), anionic ligands enter the coordination sphere of the formed complex to compensate for the charge of the central atom [32,33], in contrast to their negatively charged congeners, tris(pyrazol-1-yl)borates (TPB), for which the neutral complexes $Ln^{III}(TPB)_3$ [34–38] and $Ln^{II}(TPB)_2$ [39–41] can be assembled.

An interaction of $Eu(NO_3)_3{\cdot}5H_2O$ with a tripodal ligand in a 1:1 ratio in acetonitrile solution leads to a formation of mono-aqua complex $[Eu(HCPz_3)(NO_3)_3H_2O]{\cdot}2MeCN$ (**1**), when reacting with unsubstituted trispyrazolylmethane tripod, ($HCPz_3$); and a water free nitrate compound, $[Eu(HC(Pz^{Me_2})_3)(NO_3)_3]{\cdot}MeCN$ (**2**), upon coordination of the methylated congener of $HCPz_3$ – tris(3,5-dimethyl-1-pyrazolyl)methane. The absence of aqua–ligand in **2** is most likely due to the steric hindrance of the Pz^{Me_2}–tripod. It is worth noting that for the chloride analogue, $[Ln(HC(Pz^{Me_2})_3)Cl_3]{\cdot}2MeCN$, no water molecule were also found enter the coordination sphere upon the reaction in acetonitrile under obvious conditions [42], whereas the interaction of hydrated salt, $EuCl_3{\cdot}6H_2O$, with $HCPz_3$ in tetrahydrofuran results in a six-aqua complex – $[EuHC(Pz)_3(H_2O)_6]Cl_3$ [25].

The seven-coordinate mono-tripod complexes, $[Ln(HC(Pz^{Me_2})_3)(OTf)_3(thf)]$, where Ln = Y, Ho, Dy were formed in a dry and inert tetrahydrofuran media [32]. However, in open air, a reaction of one equivalent of europium(III) triflate with one equivalent of $HCPz_3$ in acetonitrile solution results in a dimerized entity $[Eu(HCPz_3)H_2O(CF_3SO_3)_3]_2$ (**3**), in which the central atoms are also seven-coordinate. The crystals of **3** contain the solvate molecules of acetonitrile and diethyl ether, which escape easily during storage of the compound. Interestingly, using unsubstituted anionic tripod, hydro-tris(pyrazolyl)borate ($HBPz_3$), in an inert and dry atmosphere in , the dimeric compounds $[Ln(HBPz_3)_2(CF_3SO_3)]_2$ were also obtained for Ln = Y, Eu in which the two triflates are bridged. In contrast, the molecular structures of Gd and Yb are monomeric THF-adducts $[Ln(HBPz_3)_2(CF_3SO_3)thf]$ [43].

3.2. Description of the Crystal Structures 1–3

A summary of the crystallographic data and the structure refinement is given in Table S1 (Supplementary information, SI). As established by X-ray diffraction experiment, the mononuclear compounds crystallize in the following space groups *P*–1, *I*2/*c*, and $P2_1/n$ for **1**, **1a** and **2** respectively, whereas a binuclear specie **3** – in $P2_1/c$. In all compounds, each metal central atom is capped with one neutral tripodal ligand. Among the structurally studied heteroleptic complexes, only **1a** does not have solvate molecules. **1** differs from **1a** by presence of solvate acetonitrile molecules in its crystal structure. In both compounds, a europium center has a coordination number of ten consisting of three nitrogens of trispyrazolylmethane, six oxygens of bidentate nitrate anions and one aqua–oxygen, Figure 1.

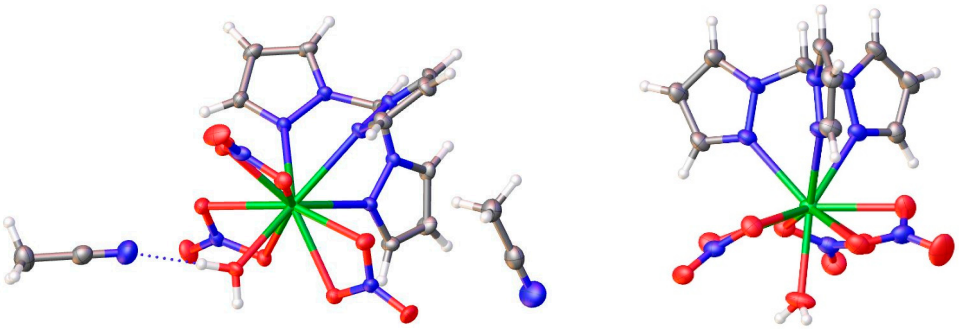

(**a**) (**b**)

Figure 1. The asymmetric units in the crystal structure of: (**a**) $[Eu(HCPz_3)(NO_3)_3H_2O]{\cdot}2MeCN$ (**1**); (**b**) $[Eu(HCPz_3)(NO_3)_3H_2O]$ (**1a**).

The Eu-N distances of **1** are in the range of 2.5810(12) to 2.5932(12) Å, which are somewhat larger than those for nitrates (2.4846(10)-2.5687(11) Å), the distance of the Eu-O_{aqua} bond of 2.4191(11) Å being a shortest one, Table 1. The same tendency is observed and for other compounds. However,

Preprints (www.preprints.org) | NOT PEER-REVIEWED | Posted: 25 August 2023 doi:10.20944/preprints202308.1806.v1

the most compact is a coordination environment of **2**, which contains one solvated acetonitrile molecule, Figure 2a. According to analysis of the 10-coordinate polyhedrons using SHAPE program [44], a geometry of the lanthanide site in **1** and **1a** can be best described as a sphenocorona (C_{2v}), while for the 9-coordinate environment of **2**, a spherical tricapped trigonal prism (D_{3h}) is more acceptable (Table S2, SI).

Table 1. The coordination polyhedron bond and Eu ···· Eu distances (Å) in the studied compounds.

	1	**1a**	**2**	**3**			
				Eu1[1]		**Eu2**[1]	
Eu—N	2.5810(12)	2.5678(16)	2.5402(19)	Eu1—N1	2.520(8)	Eu2—N7	2.533(8)
	2.5926(12)	2.5180(17)	2.5592(19)	Eu1—N3	2.537(8)	Eu2—N9	2.542(9)
	2.5932(12)	2.6072(16)	2.5158(18)	Eu1—N5	2.552(8)	Eu2—N11	2.552(9)
mean	*2.5889*	*2.5643*	*2.5384*		*5.36*		*5.42*
Eu—O$_{anion}$	2.5687(11)	2.4909(14)	2.4440(17)	Eu1—O1	2.378(6)	Eu2—O11	2.382(7)
	2.4846(10)	2.7172(16)	2.4883(17)	Eu1—O3^{i}	2.404(6)	Eu2—O14	2.520(8)
	2.5153(11)	2.4288(13)	2.4718(17)	Eu1—O4	2.376(6)	Eu2—O17	2.537(8)
	2.4655(11)	2.4983(15)	2.4465(17)	Eu1—O7	2.334(6)	Eu2—O19^{ii}	2.552(8)
	2.5234(11)	2.5306(15)	2.4674(17)	*mean*	*2.373*	*mean*	*2.498*
	2.5005(11)	2.5199(15)	2.4514(17)				
mean	*2.5097*	*2.5310*	*2.4616*				
Eu—O$_{aqua}$	2.4191(11)	2.4237(15)		Eu1—O10	2.382(7)	Eu2—O20	2.360(8)
Eu ···· Eu	6.151	6.646	8.931		6.137		6.073

[1] Symmetry codes for compound **3**: (i) −*x*+3, −*y*+2, −*z*+2; (ii) −*x*+2, −*y*+2, −*z*+2.

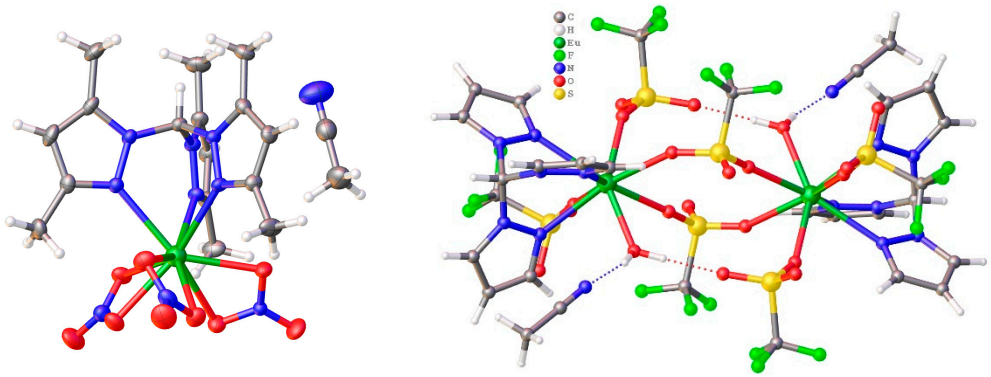

(**a**) (**b**)

Figure 2. (**a**) An asymmetric unit in the crystal structure of [Eu(HC(Pz^{Me}$_2$)$_3$)(NO$_3$)$_3$]·MeCN (**2**); (**b**) A dimer organization for Eu01 site in the crystal structure of [Eu(HCPz$_3$)H$_2$O(CF$_3$SO$_3$)$_3$]$_2$ (**3**).

Among all studied complexes **1-3**, the most intriguing is a molecular structure of **3** in which there are two independent Eu^{3+} sites with coordination number of eight (Figure S1), which is composed of three trispyrazolylmethane nitrogens, two μ_2-oxygens of bidentate triflate anions, two oxygens from monodentate triflate ligand, and one aqua–oxygen. A duplication of the corresponding independent parts via an inversion center gives two different dimeric molecules. One of them is shown in Figure 2b. In addition to the two bidentate triflate ligands, each binuclear entity is supported by two water–triflate hydrogen bonds, which are in a plane perpendicular to that in which the bridging anions are located, thus forming a Chinese lantern structure. The stereochemical analysis results indicate that the geometry of the coordination environment for both metal sites corresponds to a square antiprism (D_{4d}) to a good approximation (Figure S2, Table S2, SI). Nevertheless, despite the similar polyhedron geometry, the two Eu sites differ quite significantly in the bond lengths of europium atoms to donors being on average shorter for Eu1 (Table 1).

Preprints (www.preprints.org) | NOT PEER-REVIEWED | Posted: 25 August 2023 doi:10.20944/preprints202308.1806.v1

Crystal packing analysis shows that the shortest Eu ···· Eu distances are in the range of 6.073 ÷ 8.931 Å (Table 1). These distances have an intermolecular character only for **2**, for which no hydrogen bonds were detected, while **3** is a binuclear specie and the compounds **1** and **1a** are dimerized by double hydrogen bounding (Figure S3, SI). The distances of the shortest intermolecular contacts between a tripod and anionic ligand, $CH^{L}\cdots O_{anion}$, are 3.281, 3.245, 3.334 and 3.325 Å for **1**, **1a**, **2** and **3** respectively.

3.3. Magnetic Behavior of The Complexes

The experimental *dc* magnetic susceptibility for the complexes **1–3** measured in the temperature range from 1.77 to 300 K at the applied magnetic field $H = 1$ kOe are shown in Figure 3 as plots of $\chi_M T$ *vs.* T, where χ_M is the molar magnetic susceptibility corrected for the diamagnetic core contribution. As expected, due to the thermal depopulation of the excited levels with non-zero J values, $\chi_M T$ gradually decreases with cooling and tends to a value very close to zero as the temperature approaches absolute zero. The $\chi_M T$ values at low and room temperature for all complexes are summarized in Table 2. Below ≈ 100 K, $\chi_M T$ varies almost linearly with T (Figure 3), implying the magnetic susceptibility χ_M to be nearly temperature independent at low T. Indeed, the $\chi_M(T)$ dependencies (presented in Figure S4, SI) exhibit a smooth growth upon cooling, tending to saturate and form a plateau below ~100 K. A small increase of χ_M at very low temperatures is due to the inevitable presence of Eu^{2+} impurities (at a level of 0.01-0.017 at.%) or other rare-earth impurity ions possessing paramagnetic ground state. Subtraction of this impurity contribution recovers the intrinsic temperature-independent magnetic susceptibility of Eu^{3+} ions.

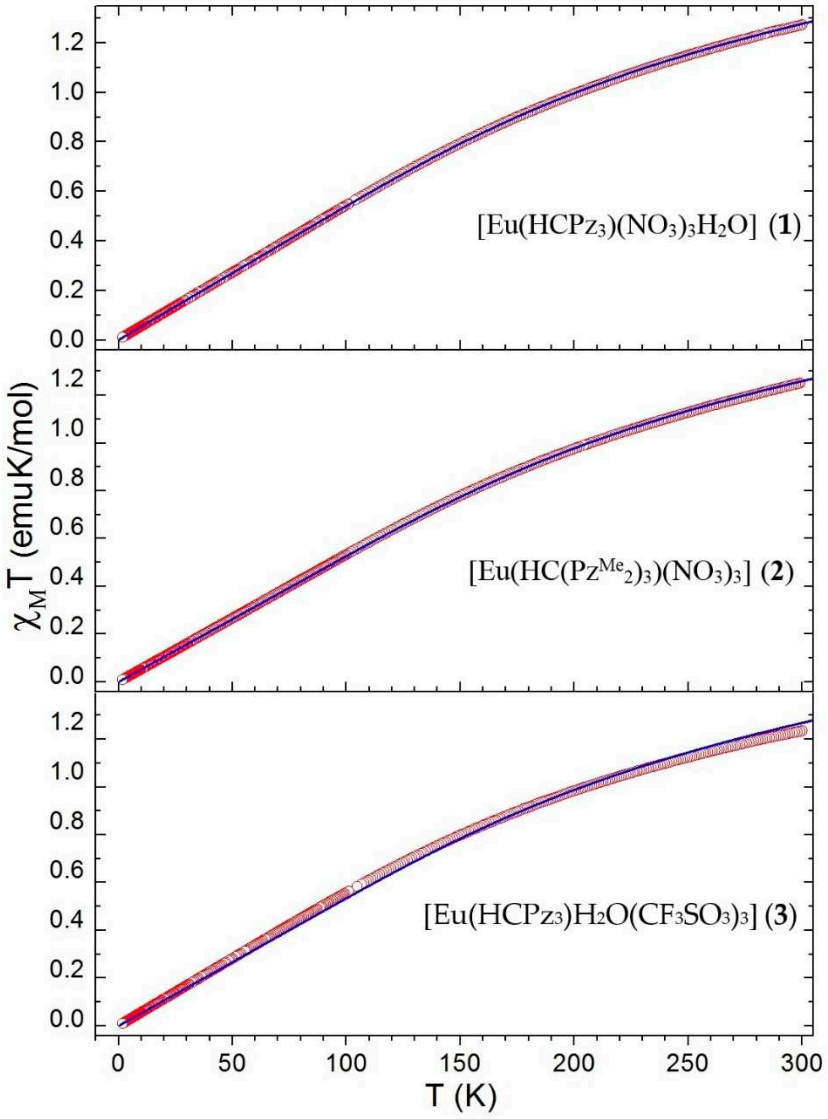

Preprints (www.preprints.org) | NOT PEER-REVIEWED | Posted: 25 August 2023 doi:10.20944/preprints202308.1806.v1

Figure 3. The $\chi_M T$ versus T data (○) measured at the applied magnetic field H = 1 kOe. The blue lines show the best fits to the data of Eq. (4) with the spin-orbit coupling λ being the only adjustable parameter; resulting values of λ are presented in Table 2.

Table 2. Magnetic parameters for europium(III) molecular compounds.

Compound	$\chi_M T$ (emu·K/mol)		λ (cm^{-1})[a]	R[b]	Reference
	2 K	300 K			
Free Eu^{3+}	0	1.280	220–380		[21,45]
1	0.0113	1.228	406	1.02×10^{-4}	this work
2	0.0114	1.251	396	4.10×10^{-5}	this work
3/Eu	0.0120	1.255	383	3.26×10^{-4}	this work
$[Eu_2(L^1)_6(H_2O)_4]_n$/Eu	0.025	1.325	343/360[c]		[46]
$[Eu_2(tzf)_3(H_2O)_6]_n$/Eu	0.020	1.388	344	2.7×10^{-4}	[47]
$[Eu_2L^2{}_6Pen_2(H_2O)_2]$/Eu			404/379[d]	3.1×10^{-4}	[48]
$[EuL^3(H_2O)_2SO_4]_n$			336	4.28×10^{-4}	[49]
$[EuL^4{}_3(CH_3OH)_3]_n$			360	9.65×10^{-5}	[50]
$[Eu_2(Hpcpa)_3(H_2O)_5]_n$	sap	1.2	356/351[c]	2.2×10^{-5}	[51]
$[Eu(HL^{Cl})_4(dmso)]^-$		1.37	348	4.1×10^{-5}	[52]
$[Eu(HL^F)_4(dmso)]^-$		1.37	336	2.1×10^{-5}	[52]
$[EuL^5{}_2(H_2O)_4](ClO_4)_3]$			362/370[c]	7.0×10^{-4}	[29]
$[Eu(^{tripp}BAP)_3]$			363		[6]
$[EuL^6PhCOO](ClO_4)_2$	0.015	1.30	370/410[d]		[53]
$[Eu(Nitrone)_2(NO_3)_3]$		1.25	371.5		[15]
$[Eu(HBPz_3)_2Trp]$	0.037	1.48			[22]
$[Eu(hfac)_3NN^e]$	0.192	1.946	332	2.0×10^{-3}	[19]
$Eu(OEP)^{2-}(OEP)^-]$	0.208	1.575			[20]
$[Eu^{III}(AP^{2-})(ISQ)^-]$	0.252	1.834			[21]
$[Eu(HBPz_3)_2SQ]$	0.28	1.59			[22]
$[Eu(hfac)_3NN_2]^{SMMTb}$	0.035	2.24	259		[12]
$[Eu(hfac)_3{}^{PhOMe}NN_2]$	0.11	1.89			[13]
$[Eu(hfac)_3NN_2]$	0.12	1.98	309		[14]
$[EuNN^{trz}{}_2(NO_3)_3]$	0.24	1.93			[15]
$[Eu(hfac)_3NN_2]$	0.419	3.09			[16]
$[Eu(hfac)_3NN_2]$		2.38	175		[17]
$[Eu(hfac)_3NN_2]$		2.12	331		[18]
$[EuRad_2(OTf)_3]$	0.348	1.78			[11]
$[Eu(hfac)_3NN^{Et}]_n$	0.89	1.9			[54]
$[Eu(hfac)_3NN]_n$		1.88	267	1.47×10^{-4}	[55]
$[Eu_2(acac)_4{}^{PhO}NN_2]$	0.66	3.47	326	2.67×10^{-5}	[56]
$[NN_4CuL_2(Eu(hfac)_3)_3]$	0.38	5.78		1.8×10^{-3}	[57]

[a] Spin-orbit coupling parameter; [b] Agreement factor; [c] Found from optic data at 77 K; [d] found from optic data at RT; [e] NN is nitronyl nitroxide type radical ligand.

The temperature dependences of $\chi_M T$ in Figure 3 can be analyzed using the van Vleck approximation (3), (4) and assuming a simplified electronic structure of Eu^{3+} ion composed of seven multiplets with energies $E(J) = \lambda J(J + 1)/2$ [29]. The least squares fitting using equation (4) with λ as the only adjustable parameter (dashed blue lines in Fig. 3) results in the λ values of ≈ 383–406 cm^{-1} for **1**-**3** (Table 2) – values typical for Eu^{3+} compounds. A common feature of all these fits that is worth mentioning is that the fits underestimate the $\chi_M T$ values in the low-temperature region where χ_M exhibits a plateau. As we have discussed in Sec.2, this feature is quite expected because the equation (4) does not take into account zero-field splitting of the excited multiplets with $J \neq 0$. The latter inevitably reduces the energy difference between the ground-state $J = 0$ level and the lowest in energy

Preprints (www.preprints.org) | NOT PEER-REVIEWED | Posted: 25 August 2023 doi:10.20944/preprints202308.1806.v1

sublevel of the J = 1 multiplet, E_1 [29–31]. In the case of strong zero-field splitting, E_1 may be significantly smaller than λ, thereby providing the low-T magnetic susceptibility to be much larger than $\chi_{LT} = 8N\beta^2/\lambda$ predicted by the equation (4) [31].

In the entire available temperature range the field dependences of the magnetization $M(H)$ demonstrate an almost perfect linear behavior (Figure 4). The magnitude of the magnetization is however 2-3 orders of magnitude lower than for other rare-earth ions with a $J \neq 0$ ground state; even at the lowest temperature T = 1.77 K the magnetization at H = 10 kOe amounts only to ≈ 0.01 μ_B per Eu^{3+} ion. These features are common to many other europium(III) complexes with diamagnetic ligands accumulated in Table 2.

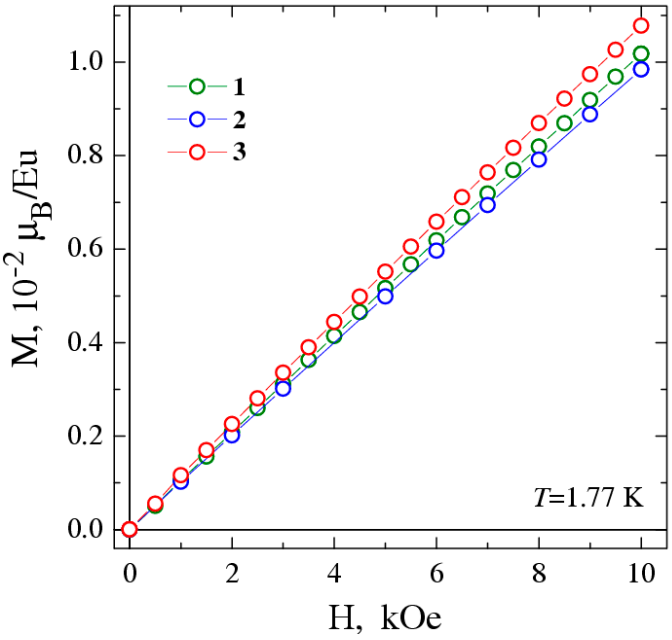

Figure 4. Field dependences of the magnetization measured for **1**-**3** at T = 1.77 K.

3.4. Spin-orbit Coupling Parameter Analysis

For all compounds, the values of R, the factors of agreement of the theoretical curves with the experimental ones, given in Table 2, indicate the applicability of the chosen qualitative model. However, for nitrate-containing complexes **1** and **2** this agreement is better compared to **3**. This is most likely due to the significant difference in the splitting of Eu^{3+} excited levels (especially of $^7F_1$ state) under the action of the crystal field.

Indeed, despite approximately the same set of donor atoms: nitrogens from a tripodal ligand and oxygens from the anion ligands, the latter, in compound **3**, have a pronounced electron withdrawing character. Whereas nitrate ligands do not possess such a property, which is confirmed by the difference in the lengths of Eu-O bonds (Table 1). In addition, despite the presence of two different europium sites in **3**, the symmetry of their local environment (D_{4d}) is higher than that of the other two: C_{2v} for **1** and D_{3h} for **2** (Table S2, SI). Based on the above, it is not surprising that simulating the experimental curve using just one variable, λ, for **3** leads to a lower-quality result compared to **1** and **2**. In addition, for a more accurate description of the high-temperature interval, it may be necessary to neglect the Eu-Eu exchange interaction, for which it may be necessary to take into account the interaction between Eu ions, by introducing into the set of variables also the coupling constant $j_{Eu\text{-}Eu}$. However, without an additional experimental data such as the luminescence spectra, the use of five independent variables would lead to overparametrization.

According to the agreement coefficients R, the modelling quality achieved is sufficient to conclude that the spin-orbit coupling parameters λ in **1** and **2** are different (by ~10 cm^{-1}). Indeed, despite the same type of tripod and anionic ligands, the coordination environment of the Eu site is significantly different for **1** and **2**, due to the presence of one water molecule in the former. Therefore,

Preprints (www.preprints.org) | NOT PEER-REVIEWED | Posted: 25 August 2023 doi:10.20944/preprints202308.1806.v1

1 has a lower symmetry of the coordination polyhedron compared to **2**, which leads to a smaller splitting of the excited levels in the crystal field. This fact is consistent with the higher value of λ: 406 for **1** *vs.* 396 cm^{-1} for **2**.

4. Experimental Section

4.1. Materials and Physical Measurements

$Ln(CF_3SO)_3$ salts (Thermo Fisher GmbH, Kandel, Germany) were purchased from Alfa Aesar. $Eu(NO_3)_3{\cdot}6H_2O$ was prepared upon dissolution of the corresponding Eu_2O_3 in diluted HNO_3 at 50°C followed by crystallization during slow evaporation of reaction mixture. Solvents of the reagent grade (EKOS-1, Moscow, Russia) were distilled prior to use. The complexes were synthesized under aerobic conditions. Elemental (C, H, N, S) analyses were carried out by standard methods with a Euro-Vector 3000 analyzer (Eurovector, Redavalle, Italy).

Magnetic measurements were performed using a Quantum Design MPMS-XL SQUID magnetometer in the temperature range of 1.77–300 K at magnetic fields up to 10 kOe. In order to determine the paramagnetic component of the molar magnetic susceptibility, $\chi_M T(T)$, the temperature-independent diamagnetic contribution, χ_d, and a possible magnetization of ferromagnetic micro-impurities, $\chi_{FM}(T)$, were evaluated and subtracted from the measured values of the total molar susceptibility, $\chi = M/H$. The diamagnetic intrinsic contributions of the compounds χ_d were estimated using the Pascal's Constants [58]. Fourier transform infrared (FTIR) spectra were measured in KBr pellets with a Perkin–Elmer System 2000 FTIR spectrometer (Perkin Elmer, Waltham, MA, USA) in the 4000–400 cm^{-1} range.

4.2. Single-crystal XRD experiment and data refinment details

Single-crystal XRD data for crystals of the compounds were collected at 150 K with a Bruker D8 Venture diffractometer (0.5° ω- and φ-scans, fixed-χ three circle goniometer, CMOS PHOTON III detector, IμS 3.0 micro-focus source, focusing Montel mirrors, λ = 0.71073 Å MoK_α radiation, N_2-flow thermostat). Data reduction was performed routinely via APEX 3 suite [59]. The crystal structures were solved using the ShelXT [60] and were refined using ShelXL [61] programs assisted by Olex2 GUI [62]. Atomic displacements for non-hydrogen atoms were refined in harmonic anisotropic approximation, with the exception for partially occupied diethyl ether molecule in **3**. Hydrogen atoms were located geometrically with the exception for those in water molecules in **1** and **1a**, which were refined freely with the restraints on O–H bond. All hydrogens were placed in geometrically idealized positions, and refined in a riding model. Crystals of compound **3** tend to form twins; as a result, the quality of the structure is lower than in the others. The structures of were deposited to the Cambridge Crystallographic Data Centre (CCDC) as a supplementary publication, No. 2285187-2285190.

4.3. Synthesis of the Complexes

*$[Eu(HCPz_3)(NO_3)_3H_2O]{\cdot}2MeCN$ (**1**)* A solution of trispyrazolylmethane (64.5 mg, 0.3 mmol) in acetonitrile (0.5 mL) was added dropwise to a stirred warm solution of $Eu(NO_3)_3(H_2O)_5$ (128 mg, 0.3 mmol) in acetonitrile (0.5 mL). The next day, the crystalline colorless precipitate was filtered, washed with a small amount of acetonitrile, and Et_2O and air-dried. Yield: 158 mg (81%) (652.32 g/mol). Storage of the compound resulted in unsolvated **1**. Anal. calcd. (%) for $C_{10}H_{12}EuN_9O_{10}$: C, 21.02; H, 2.12; N, 22.07. Found: C, 21.1; H, 2.0; N, 22.1. IR (KBr): ν (cm^{-1}) 3423 (m), 3115 (m), 3111 (m), 2505 m, 2427 (sh), 1507 (s), 1384 (s), 1317 (s), 1285 (s), 1230 (m),1148 (s), 1186 (s), 1148 (s), 1136 (s), 1119 (m), 1042 (m), 1028 (m), 1009 (m), 981 (m), 963 (m), 904 (m), 876 (m), 730 (s), 723 (s), 672 (s), 664 (s), 651 (m).

*$[Eu(HCPz_3)(NO_3)_3H_2O]$ (**1a**).* The mother liquor combined with flushing liquids (the both left after synthesis of **1** were evaporated to dryness. The white powder formed (30 mg) was dissolved in hot dry acetonitrile (2 mL). After filtration, the filtrate was left in a refrigerator at a temperature of 4 C during one week. The colorless crystals were filtered, rinsed with a small amount of cold

acetonitrile and air-dried. Yield: 17 mg (570.22 g/mol); Anal. calcd. (%) for $C_{10}H_{12}EuN_9O_{10}$: C, 21.02; H, 2.12; N, 22.07. Found: C, 21.2; H, 2.1; N, 22.0. I. IR (KBr) is similar to that of **1**.

*[Eu(HC(Pz^{Me_2})$_3$)(NO$_3$)$_3$]·MeCN (**2**)* To a stirred and hot solution of the metal salt (84 mg (0.2 mmol) of $Eu(NO_3)_3(H_2O)_5$) in acetonitrile (1.5 mL), solid tris(3,5-dimethyl-1-pyrazolyl)methane (60 mg, 0.2 mmol) was gradually added under heating. The solution was filtered and kept at room temperature overnight, and then the resulting colorless crystalline solid was sucked off, washed twice with cold acetonitrile and air-dried. Yield: 112 mg (84 %) (677.41 g/mol). Storage of the compound resulted in unsolvated **3**. Anal. calcd. (%) for $C_{16}H_{22}EuN_9O_9$: C, 30.14; H, 3.48; N, 19.65. Found C, 30.2; H, 3.3; N, 19.65. IR (KBr) ν (cm^{-1}) : 487 (m); 636 (w); 707 (s); 746 (s); 802 (m); 811 (s); 822 (w); 836 (m); 859 (s); 864 (s); 906 (s); 983 (m); 1024 (s); 1042 (s); 1109 (m); 1153 (w); 1169 (w); 1276 (s); 1304 (s); 1417 (m); 1515 (s); 1530 (m); 1570 (s); 1732 (w); 1771 (w); 1977 (w); 2043 (w); 2268 (m); 2292 (w); 2533 (w).

*[Eu(HCPz$_3$)H$_2$O(CF$_3$SO$_3$)$_3$]$_2$·2MeCN·0.73Et$_2$O (**3**).* A solution of trispyrazolylmethane (54 mg, 0.25 mmol) in acetonitrile (1 mL) was added dropwise to a stirred solution of $Eu(CF_3SO_3)_3$·(150 mg, 0.25 mmol) in acetonitrile (2 mL). The reaction mixture was halved by heating (65 C) and slowly cooled to room temperature, and then left undisturbed overnight in a closed vessel with a few drops of Et_2O. The crystalline colorless solid was filtered, washed with a small amount of acetonitrile, and Et_2O and air-dried. Yield: 209 mg (45%) $C_{32.9}H_{37.24}Eu_2F_{18}N_{14}O_{20.73}S_6$ (1798.66 g/mol). Storage of the compound resulted in unsolvated **4**. Anal. calcd. (%) for $C_{26}H_{24}Eu_2F_{18}S_6N_{12}O_{20}$ (1662.8 g/mol): Anal. calcd. (%): C, 18.78, H, 1.45, N, 10.11; S, 11.7; found: C, 18.6, H, 1.6, N, 10.0; S, 11.5. IR (KBr) ν (cm^{-1}) : 3140 (w); 3130 (w); 1578 (m); 1549 (m); 1527 (m); 1409 (m); 1292 (s); 1200 (s); 1166 (s); 1110 (m); 1094 (m); 1029 (m); 960 (m); 920 (m); 889 (m); 857 (m); 824 (m); 810 (m); 755 (s); 722 (m); 638 (s); 597 (m); 574 (m); 517 (m); 410 (w); 389 (w); 351 (w).

5. Conclusions and perspectives

In the absence of analytical models accounting for strong spin-orbit coupling for Eu^{3+} complexes with paramagnetic ligands, alternative approaches are needed to determine the nature and magnitude of the exchange coupling between paramagnetic centers in such complicated systems. The proposed earlier solution, based on subtraction from the experimental dependence of the magnetic susceptibility, $\chi_M(T)$, for a series of lanthanide complexes with radicals [15,23] the same dependence of the model compound of the corresponding Ln with a diamagnetic ligand possessing a similar coordination polyhedron geometry turned out to be particularly effective for [Ln(HBPz$_3$)$_2$SQ] [23].

In the present study, we were able to find a model system, [Ln(HC(Pz^{Me_2})$_3$)(NO$_3$)$_3$], for monoradical complexes [LnRad(NO$_3$)$_3$] since both types of compounds have the same type of coordination polyhedron and very close Ln – donor atoms distances. It is quite possible that the neutral ligand HC(Pz^{Me_2})$_3$ can also be used for the synthesis of bis-tripodal complexes [Ln(HC(Pz^{Me_2})$_3$)$_2$](anion)$_3$ as model systems for biradical compounds with sterically hindered paramagnetic tripods [Ln(Rad)^{Me_2}](anion)$_3$, for which the corresponding ligands are under preparation. As surprising as it may be, the homoleptic Ln^{3+} complexes involving two balky diamagnetic tripods of type HC(Pz^{Me_2})$_3$ in their composition are still unknown. Consequently, developing methods to synthesize them is a particular challenge.

Author Contributions: Conceptualization, K.E.V.; funding acquisition, K.E.V.; investigation, K.E.V., V.S.M. and E.V.P.; supervision K.E.V.; visualization, K.E.V. and V.S.M.; writing—original draft, K.E.V., V.S.M. and E.V.P.; writing—review and editing, K.E.V., V.S.M. and E.V.P. All authors have read and agreed to the published version of the manuscript.

Supplementary Materials: The following supporting information can be downloaded at: www.mdpi.com/xxx/s1, Table S1: Crystal data and structure refinement for the compounds; Figure S1: The asymmetric unit in the crystal structure of [Eu(HCPz$_3$)H$_2$O(CF$_3$SO$_3$)$_3$]$_2$ (3); Figure S2: Square antiprism coordination environment - of Eu^{3+} sites in [Eu(HCPz$_3$)H$_2$O(CF$_3$SO$_3$)$_3$]$_2$ (3) for: (a) around Eu1 central atom, (b) around Eu2 central atom; Table S2: Geometry analysis of the complexes by SHAPE software; Figure S3: Dimerized species in 1 (left) and 1a (right); Figure S4: The temperature-dependent molar magnetic susceptibility for 1–3 measured at a field of 1 kOe in the 1.8–300 K temperature range.

Author Contributions: Conceptualization, K.E.V. and A.N.L.; methodology, K.E.V.; software, T.S.S.; formal analysis, T.S.S.; investigation, K.E.V. and A.N.L.; resources, X.X.; data curation, T.S.S.; writing—original draft preparation, K.E.V.; writing—review and editing, K.E.V. and A.N.L.; visualization, K.E.V. and A.N.L.; supervision, K.E.V.; funding acquisition, K.E.V. All authors have read and agreed to the published version of the manuscript.

Funding: This research was funded by Russian Science Foundation, Grant No. 23-23-00437, and partially supported by the Ministry of Science and Higher Education of the Russian Federation (crystal structure determination for the complexes, 121031700313-8).

Institutional Review Board Statement: Not applicable.

Informed Consent Statement: Not applicable.

Data Availability Statement: CCDC 2285187-2285190 for **1–4** contain the supplementary crystallographic data for this paper, and can be obtained free of charge from The Cambridge Crystallographic Data Centre via **https://www.ccdc.cam.ac.uk/structures/** (accessed on 31 July 2023).

Acknowledgments: In this section, you can acknowledge any support given which is not covered by the author contribution or funding sections.

Conflicts of Interest: The authors declare no conflict of interest.

References

1. Yi, X.; Bernot, K.; Pointillart, F.; Poneti, G.; Calvez, G.; Daiguebonne, C.; Guillou, O.; Sessoli, R. A Luminescent and Sublimable Dy^{III}-Based Single-Molecule Magnet. *Chem. – A Eur. J.* **2012**, *18*, 11379–11387, doi: 10.1002/chem.201201167.
2. Marin, R.; Brunet, G.; Murugesu, M. Shining New Light on Multifunctional Lanthanide Single-Molecule Magnets. *Angew. Chemie Int. Ed.* **2021**, *60*, 1728–1746, doi:https://doi.org/10.1002/anie.201910299.
3. Suta, M.; Wickleder, C. Synthesis, Spectroscopic Properties and Applications of Divalent Lanthanides Apart from Eu2+. *J. Lumin.* **2019**, *210*, 210–238, doi:https://doi.org/10.1016/j.jlumin.2019.02.031.
4. Morss, L.R.B.T.-H. on the P. and C. of R.E. Chapter 122 Comparative Thermochemical and Oxidation-Reduction Properties of Lanthanides and Actinides. In *Lanthanides/Actinides: Chemistry*; Elsevier, 1994; Vol. 18, pp. 239–291 ISBN 0168-1273.
5. Rodrigues, L.C.V.; Hölsä, J.; Brito, H.F.; Maryško, M.; Matos, J.R.; Paturi, P.; Rodrigues, R. V.; Lastusaari, M. Magneto-Optical Studies of Valence Instability in Europium and Terbium Phosphors. *J. Lumin.* **2016**, *170*, 701–706, doi:10.1016/j.jlumin.2015.08.018.
6. Chen, J.; Carpenter, S.H.; Fetrow, T. V.; Mengell, J.; Kirk, M.L.; Tondreau, A.M. Magnetism Studies of Bis(Acyl)Phosphide-Supported Eu^{3+} and Eu^{2+} Complexes. *Inorg. Chem.* **2022**, *61*, 18466–18475, doi:10.1021/acs.inorgchem.2c02675.
7. Evans, W.J. Perspectives in Reductive Lanthanide Chemistry. *Coord. Chem. Rev.* **2000**, *206–207*, 263–283, doi:https://doi.org/10.1016/S0010-8545(00)00267-8.
8. Dolai, M.; Ali, M.; Rajnák, C.; Titiš, J.; Boča, R. Slow Magnetic Relaxation in Cu(II)–Eu(III) and Cu(II)–La(III) Complexes. *New J. Chem.* **2019**, *43*, 12698–12701, doi:10.1039/C9NJ02039J.
9. Wang, J.; Ruan, Z.-Y.; Li, Q.-W.; Chen, Y.-C.; Huang, G.-Z.; Liu, J.-L.; Reta, D.; Chilton, N.F.; Wang, Z.-X.; Tong, M.-L. Slow Magnetic Relaxation in a $\{EuCu_5\}$ Metallacrown. *Dalt. Trans.* **2019**, *48*, 1686–1692, doi:10.1039/C8DT04814B.
10. Perfetti, M.; Caneschi, A.; Sukhikh, T.S.; Vostrikova, K.E. Lanthanide Complexes with a Tripodal Nitroxyl Radical Showing Strong Magnetic Coupling. *Inorg. Chem.* **2020**, *59*, 16591–16598, doi:10.1021/acs.inorgchem.0c02477.
11. Rey, P.; Caneschi, A.; Sukhikh, T.S.; Vostrikova, K.E. Tripodal Oxazolidine-N-Oxyl Diradical Complexes of Dy^{3+} and Eu^{3+}. *Inorganics* **2021**, *9*, 91, doi:10.3390/inorganics9120091.
12. Tretyakov, E. V; Fokin, S. V; Zueva, E.M.; Tkacheva, A.O.; Romanenko, G. V; Bogomyakov, A.S.; Larionov, S. V; Popov, S.A.; Ovcharenko, V.I. Complexes of Lanthanides with Spin-Labeled Pyrazolylquinoline. *Russ. Chem. Bull.* **2014**, *63*, 1459–1464, doi:10.1007/s11172-014-0621-8.
13. Wang, X.; Li, Y.; Hu, P.; Wang, J.; Li, L. Slow Magnetic Relaxation and Field-Induced Metamagnetism in Nitronyl Nitroxide-Dy(III) Magnetic Chains. *Dalt. Trans.* **2015**, *44*, 4560–4567, doi:10.1039/C4DT01878H.
14. Wang, Y.; Fan, Z.; Yin, X.; Wang, S.; Yang, S.; Zhang, J.; Geng, L.; Shi, S. Structure and Magnetic Investigation of a Series of Rare Earth Heterospin Monometallic Compounds of Nitronyl Nitroxide Radical. *Zeitschrift für Anorg. und Allg. Chemie* **2016**, *642*, 148–154, doi:https://doi.org/10.1002/zaac.201500644.
15. Kahn, M.L.; Sutter, J.-P.; Golhen, S.; Guionneau, P.; Ouahab, L.; Kahn, O.; Chasseau, D. Systematic Investigation of the Nature of the Coupling between a Ln(III) Ion (Ln = Ce(III) to Dy(III)) and Its Aminoxyl Radical Ligands. Structural and Magnetic Characteristics of a Series of $\{Ln(Radical)_2\}$ Compounds and the Related $\{Ln(Nitrone)_2\}$ Derivat. *J. Am. Chem. Soc.* **2000**, *122*, 3413–3421, doi:10.1021/ja994175o.

16. Lv, X.-H.; Yang, S.-L.; Li, Y.-X.; Zhang, C.-X.; Wang, Q.-L. A Family of Lanthanide Compounds Based on Nitronyl Nitroxide Radicals: Synthesis, Structure, Magnetic and Fluorescence Properties. *RSC Adv.* **2017**, *7*, 38179–38186, doi:10.1039/C7RA05764D.
17. Fan, Z.; Hou, Y.-F.; Wang, S.-P.; Yang, S.-T.; Zhang, J.-J.; Shi, S.-K.; Geng, L.-N. Synthesis, Crystal Structure, and Magnetic Property of New Trispin Ln(III)-Nitronyl Nitroxide Complexes. *Helv. Chim. Acta* **2016**, *99*, 732–741, doi:https://doi.org/10.1002/hlca.201600152.
18. Wang, Y.-L.; Gao, Y.-Y.; Ma, Y.; Wang, Q.-L.; Li, L.-C.; Liao, D.-Z. Syntheses, Crystal Structures, Magnetic and Luminescence Properties of Five Novel Lanthanide Complexes of Nitronyl Nitroxide Radical. *J. Solid State Chem.* **2013**, *202*, 276–281, doi:https://doi.org/10.1016/j.jssc.2013.03.052.
19. Xu, J.-X.; Ma, Y.; Liao, D.; Xu, G.-F.; Tang, J.; Wang, C.; Zhou, N.; Yan, S.-P.; Cheng, P.; Li, L.-C. Four New Lanthanide−Nitronyl Nitroxide (Ln^{III} = Pr^{III}, Sm^{III}, Eu^{III}, Tm^{III}) Complexes and a Tb^{III} Complex Exhibiting Single-Molecule Magnet Behavior. *Inorg. Chem.* **2009**, *48*, 8890–8896, doi:10.1021/ic901169p.
20. Buchler, J.W.; De Cian, A.; Fischer, J.; Kihn-Botulinski, M.; Weiss, R. Metal Complexes with Tetrapyrrole Ligands. 46. Europium(III) Bis(Octaethylporphyrinate), a Lanthanoid Porphyrin Sandwich with Porphyrin Rings in Different Oxidation States, and Dieuropium(III) Tris(Octaethylporphyrinate). *Inorg. Chem.* **1988**, *27*, 339–345, doi:10.1021/ic00275a022.
21. Klementyeva, S. V.; Gritsan, N.P.; Khusniyarov, M.M.; Witt, A.; Dmitriev, A.A.; Suturina, E.A.; Hill, N.D.D.; Roemmele, T.L.; Gamer, M.T.; Boeré, R.T.; et al. The First Lanthanide Complexes with a Redox-Active Sulfur Diimide Ligand: Synthesis and Characterization of $[LnCp^*_2(RN{=})_2S]$, Ln=Sm, Eu, Yb; R=SiMe3. *Chem. - A Eur. J.* **2017**, *23*, 1278–1290, doi:10.1002/chem.201604340.
22. Caneschi, A.; Dei, A.; Gatteschi, D.; Poussereau, S.; Sorace, L. Antiferromagnetic Coupling between Rare Earth Ions and Semiquinones in a Series of 1 ： 1 Complexes. *Dalt. Trans.* **2004**, 1048–1055, doi:10.1039/B401144A.
23. Dei, A.; Gatteschi, D.; Pécaut, J.; Poussereau, S.; Sorace, L.; Vostrikova, K. Crystal Field and Exchange Effects in Rare Earth Semiquinone Complexes. *Comptes Rendus l'Academie des Sci. - Ser. IIC Chem.* **2001**, *4*, doi:10.1016/S1387-1609(00)01196-8.
24. Gaft, M.; Reisfeld, R.; Panczer, G. *Modern Luminescence Spectroscopy of Minerals and Materials*; Springer-Verlag: Berlin/Heidelberg, 2005; ISBN 3-540-21918-8.
25. Machado, K.; Mukhopadhyay, S.; Videira, R.A.; Mishra, J.; Mobin, S.M.; Mishra, G.S. Polymer Encapsulated Scorpionate Eu^{3+} Complexes as Novel Hybrid Materials for High Performance Luminescence Applications. *RSC Adv.* **2015**, *5*, 35675–35682, doi:10.1039/C5RA02866C.
26. Binnemans, K. Interpretation of Europium(III) Spectra. *Coord. Chem. Rev.* **2015**, *295*, 1–45, doi:10.1016/j.ccr.2015.02.015.
27. Bünzli, J.-C.G. On the Design of Highly Luminescent Lanthanide Complexes. *Coord. Chem. Rev.* **2015**, *293–294*, 19–47, doi:https://doi.org/10.1016/j.ccr.2014.10.013.
28. Sorace, L.; Gatteschi, D. Electronic Structure and Magnetic Properties of Lanthanide Molecular Complexes. In *Lanthanides and Actinides in Molecular Magnetism*; Wiley-VCH Verlag GmbH & Co. KGaA: Weinheim, Germany, 2015; pp. 1–26.
29. Andruh, M.; Bakalbassis, E.; Kahn, O.; Trombe, J.C.; Porcher, P. Structure, Spectroscopic and Magnetic Properties of Rare Earth Metal(III) Derivatives with the 2-Formyl-4-Methyl-6-(N-(2-Pyridylethyl)Formimidoyl)Phenol Ligand. *Inorg. Chem.* **1993**, *32*, 1616–1622, doi:10.1021/ic00061a017.
30. Huang, J.; Loriers, J.; Porcher, P.; Teste de Sagey, G.; Caro, P.; Levy-Clement, C. Crystal Field Effect and Paramagnetic Susceptibility of $Na_5Eu(MoO_4)_4$ and $Na_5Eu(WO_4)_4$. *J. Chem. Phys.* **1984**, *80*, 6204–6209, doi:10.1063/1.446723.
31. Caro, P.; Porcher, P. The Paramagnetic Susceptibility of C-Type Europium Sesquioxide. *J. Magn. Magn. Mater.* **1986**, *58*, 61–66, doi:10.1016/0304-8853(86)90123-X.
32. Sella, A.; Brown, S.E.; Steed, J.W.; Tocher, D.A. Synthesis and Solid-State Structures of Pyrazolylmethane Complexes of the Rare Earths. *Inorg. Chem.* **2007**, *46*, 1856–1864, doi:10.1021/ic062370f.
33. Chen, S.-J.; Li, Y.-Z.; Chen, X.-T.; Shi, Y.-J.; You, X.-Z. Tetrabutylammonium Tetrakis(Nitrato-κ2O,O′)[1,3,5-Tris(Pyrazolyl) Methane-κ3N]Cerate(III). *Acta Crystallogr. Sect. E Struct. Reports Online* **2002**, *58*, m753–m755, doi:10.1107/S1600536802021177.
34. Bagnall, K.W.; Tempest, A.C.; Takats, J.; Masino, A.P. Lanthanoid Poly(Pyrazol-1-yl) Borate Complexes. *Inorg. Nucl. Chem. Lett.* **1976**, *12*, 555–557, doi:https://doi.org/10.1016/0020-1650(76)80021-9.
35. Stainer, M.V.R.; Takats, J. X-Ray Crystal and Molecular Structure of Tris[Hydridotris(Pyrazol-1-yl)Borato]Ytterbium(III), $Yb(HBPz_3)_3$. *Inorg. Chem.* **1982**, *21*, 4050–4053, doi:10.1021/ic00141a034.
36. Apostolidis, C.; Rebizant, J.; Kanellakopulos, B.; von Ammon, R.; Dornberger, E.; Müller, J.; Powietzka, B.; Nuber, B. Homoscorpionates (Hydridotris(1-Pyrazolyl)Borato Complexes) of the Trivalent 4fions. The Crystal and Molecular Structure of $[(HB(N_2C_3H_3)_3]_3Ln^{III}$, (Ln = Pr, Nd). *Polyhedron* **1997**, *16*, 1057–1068, doi:https://doi.org/10.1016/S0277-5387(96)00391-9.
37. Apostolidis, C.; Rebizant, J.; Walter, O.; Kanellakopulos, B.; Reddmann, H.; Amberger, H.-D. Zur Elektronenstruktur Hochsymmetrischer Verbindungen Der F-Elemente. 35 [1] Kristall- Und

Molekülstrukturen von Tris(Hydrotris(1-Pyrazolyl)Borato)-Lanthanid(III) ($LnTp_3$; Ln = La, Eu) Sowie Elektronenstruktur von $EuTp_3$. *Zeitschrift für Anorg. und Allg. Chemie* **2002**, *628*, 2013–2025, doi:10.1002/1521-3749(200209)628:9/10<2013::AID-ZAAC2013>3.0.CO;2-K.

38. Apostolidis, C.; Kovács, A.; Morgenstern, A.; Rebizant, J.; Walter, O. Tris-{Hydridotris(1-Pyrazolyl)Borato}lanthanide Complexes: Synthesis, Spectroscopy, Crystal Structure and Bonding Properties. *Inorganics* **2021**, *9*, 44, doi:10.3390/inorganics9060044.
39. Reger, D.L.; Knox, S.J.; Lindeman, J.A.; Lebioda, L. Poly(Pyrazolyl) Borate Complexes of Terbium, Samarium, and Erbium. X-Ray Crystal Structure of $\{[\eta^3\text{-}HB(Pz)_3]_2Sm(\mu\text{-}O_2CPh)\}_2$ (Pz = Pyrazolyl Ring). *Inorg. Chem.* **1990**, *29*, 416–419, doi:10.1021/ic00328a015.
40. Chowdhury, T.; Evans, M.J.; Coles, M.P.; Bailey, A.G.; Peveler, W.J.; Wilson, C.; Farnaby, J.H. Reduction Chemistry Yields Stable and Soluble Divalent Lanthanide Tris(Pyrazolyl)Borate Complexes. *Chem. Commun.* **2023**, *59*, 2134–2137, doi:10.1039/D2CC03189B.
41. Qi, H.; Zhao, Z.; Zhan, G.; Sun, B.; Yan, W.; Wang, C.; Wang, L.; Liu, Z.; Bian, Z.; Huang, C. Air Stable and Efficient Rare Earth Eu(II) Hydro-Tris(Pyrazolyl)Borate Complexes with Tunable Emission Colors. *Inorg. Chem. Front.* **2020**, *7*, 4593–4599, doi:10.1039/D0QI00762E.
42. Long, J.; Lyubov, D.M.; Mahrova, T. V.; Cherkasov, A. V.; Fukin, G.K.; Guari, Y.; Larionova, J.; Trifonov, A.A. Synthesis, Structure and Magnetic Properties of Tris(Pyrazolyl)Methane Lanthanide Complexes: Effect of the Anion on the Slow Relaxation of Magnetization. *Dalt. Trans.* **2018**, *47*, 5153–5156, doi:10.1039/C8DT00458G.
43. Chowdhury, T.; Horsewill, S.J.; Wilson, C.; Farnaby, J.H. Heteroleptic Lanthanide(III) Complexes: Synthetic Utility and Versatility of the Unsubstituted Bis-Scorpionate Ligand Framework. *Aust. J. Chem.* **2022**, *75*, 660–675.
44. Llunell, M.; Casanova, D.; Cirera, J.; Alemany, P.; Alvarez, S. SHAPE, Version 2.1, Program for the Stereochemical Analysis of Molecular Fragments by Means of Continuous Shape Measures and Associated Tools. *Univ. Barcelona, Barcelona, Spain* **2013**, *2103*.
45. Rousset, E.; Piccardo, M.; Gable, R.W.; Massi, M.; Sorace, L.; Soncini, A.; Boskovic, C. Elucidation of LMCT Excited States for Lanthanoid Complexes: A Theoretical and Solid-State Experimental Framework. *Inorg. Chem.* **2022**, doi:10.1021/acs.inorgchem.2c01985.
46. Arauzo, A.; Lazarescu, A.; Shova, S.; Bartolomé, E.; Cases, R.; Luzón, J.; Bartolomé, J.; Turta, C. Structural and Magnetic Properties of Some Lanthanide (Ln = Eu^{III}, Gd^{III} and Nd^{III}) Cyanoacetate Polymers: Field-Induced Slow Magnetic Relaxation in the Gd and Nd Substitutions. *Dalt. Trans.* **2014**, *43*, 12342–12356, doi:10.1039/C4DT01104J.
47. Wu, M.-F.; Wang, M.-S.; Guo, S.-P.; Zheng, F.-K.; Chen, H.-F.; Jiang, X.-M.; Liu, G.-N.; Guo, G.-C.; Huang, J.-S. Photoluminescent and Magnetic Properties of a Series of Lanthanide Coordination Polymers with 1-H-Tetrazolate-5-Formic Acid. *Cryst. Growth Des.* **2011**, *11*, 372–381, doi:10.1021/cg100817s.
48. Li, Y.; Zheng, F.-K.; Liu, X.; Zou, W.-Q.; Guo; Lu, C.-Z.; Huang, J.-S. Crystal Structures and Magnetic and Luminescent Properties of a Series of Homodinuclear Lanthanide Complexes with 4-Cyanobenzoic Ligand. *Inorg. Chem.* **2006**, *45*, 6308–6316, doi:10.1021/ic0602603.
49. Xu, N.; Wang, C.; Shi, W.; Yan, S.-P.; Cheng, P.; Liao, D.-Z. Magnetic and Luminescent Properties of Sm, Eu, Tb, and Dy Coordination Polymers with 2-Hydroxynicotinic Acid. *Eur. J. Inorg. Chem.* **2011**, *2011*, 2387–2393, doi: 10.1002/ejic.201100022.
50. Han, M.; Li, S.; Ma, L.; Yao, B.; Feng, S.-S.; Zhu, M. Luminescent and Magnetic Bifunctional Coordination Complex Based on a Chiral Tartaric Acid Derivative and Europium. *Acta Crystallogr. Sect. C Struct. Chem.* **2019**, *75*, 1220–1227, doi:10.1107/S205322961901060X.
51. De Oliveira Maciel, J.W.; Lemes, M.A.; Valdo, A.K.; Rabelo, R.; Martins, F.T.; Queiroz Maia, L.J.; de Santana, R.C.; Lloret, F.; Julve, M.; Cangussu, D. Europium(III), Terbium(III), and Gadolinium(III) Oxamato-Based Coordination Polymers: Visible Luminescence and Slow Magnetic Relaxation. *Inorg. Chem.* **2021**, *60*, 6176–6190, doi:10.1021/acs.inorgchem.0c03226.
52. Vaz, R.C.A.; Esteves, I.O.; Oliveira, W.X.C.; Honorato, J.; Martins, F.T.; Marques, L.F.; dos Santos, G.L.; Freire, R.O.; Jesus, L.T.; Pedroso, E.F.; et al. Mononuclear Lanthanide(III)-Oxamate Complexes as New Photoluminescent Field-Induced Single-Molecule Magnets: Solid-State Photophysical and Magnetic Properties. *Dalt. Trans.* **2020**, *49*, 16106–16124, doi:10.1039/D0DT02497J.
53. Shintoyo, S.; Fujinami, T.; Matsumoto, N.; Tsuchimoto, M.; Weselski, M.; Bieńko, A.; Mrozinski, J. Synthesis, Crystal Structure, Luminescent and Magnetic Properties of Europium(III) and Terbium(III) Complexes with a Bidentate Benzoate and a Tripod N_7 Ligand Containing Three Imidazole, $[Ln^{III}(H_3L)Benzoate](ClO_4)_2{\cdot}H_2O{\cdot}2MeOH$ (Ln^{III}=Eu^{III} and Tb^{III}). *Polyhedron* **2015**, *91*, 28–34, doi:https://doi.org/10.1016/j.poly.2015.02.020.
54. Benelli, C.; Caneschi, A.; Gatteschi, D.; Pardi, L.; Rey, P. Structure and Magnetic Properties of Linear-Chain Complexes of Rare-Earth Ions (Gadolinium, Europium) with Nitronyl Nitroxides. *Inorg. Chem.* **1989**, *28*, 275–280, doi:10.1021/ic00301a024.

55. Liu, R.; Zhao, S.; Xiong, C.; Xu, J.; Li, Q.; Fang, D. Three New One-Dimensional Lanthanide Complexes Bridged by Nitronyl Nitroxide Radicals: Crystal Structures and Magnetic Characterization. *J. Mol. Struct.* **2013**, *1036*, 107–110, doi:https://doi.org/10.1016/j.molstruc.2012.09.034.
56. Mei, X.; Wang, X.; Wang, J.; Ma, Y.; Li, L.; Liao, D. Dinuclear Lanthanide Complexes Bridged by Nitronyl Nitroxide Radical Ligands with 2-Phenolate Groups: Structure and Magnetic Properties. *New J. Chem.* **2013**, *37*, 3620–3626, doi:10.1039/C3NJ00739A.
57. Zhu, M.; Jia, L.; Li, Y.; Li, Y.; Zhang, L.; Zhang, W.; Lü, Y. Nitronyl Nitroxide Bridged 3d–4f Hetero-Tri-Spin Chains: Synthesis Strategy, Crystal Structure and Magnetic Properties. *CrystEngComm* **2018**, *20*, 420–431, doi:10.1039/C7CE01962A.
58. Bain, G.A.; Berry, J.F. Diamagnetic Corrections and Pascal's Constants. *J. Chem. Educ.* **2008**, *85*, 532, doi:10.1021/ed085p532.
59. Apex3 Software Suite: Apex3, SADABS-2016/2 and SAINT 8.40a; Publisher: Bruker AXS Inc. 2017.
60. Sheldrick, G.M. SHELXT – Integrated Space-Group and Crystal-Structure Determination. *Acta Crystallogr. Sect. A Found. Adv.* **2015**, *71*, 3–8, doi:10.1107/S2053273314026370.
61. Sheldrick, G.M. Crystal Structure Refinement with SHELXL. *Acta Crystallogr. Sect. C Struct. Chem.* **2015**, *71*, 3–8, doi:10.1107/S2053229614024218.
62. Dolomanov, O. V.; Bourhis, L.J.; Gildea, R.J.; Howard, J.A.K.; Puschmann, H. OLEX2 : A Complete Structure Solution, Refinement and Analysis Program. *J. Appl. Crystallogr.* **2009**, *42*, 339–341, doi:10.1107/S0021889808042726.